Proceedings of the ASME 2023
International Mechanical Engineering Congress and Exposition
IMECE2023
October 29-November 02, 2023, New Orleans, LA, USA

IMECE2023-112803

SEPARATION OF CTCS FROM BLOOD CELLS USING CURVED CONTRACTION-EXPANSION MICROCHANNEL EQUIPPED WITH DEP FORCE

Md Tanbir Sarowar[1], Md Sadiqul Islam[2], and Xiaolin Chen[1]

[1]Washington State University Vancouver, Vancouver, WA 98686
[2]Purdue University, 585 Purdue Mall, West Lafayette, IN 47907

ABSTRACT

The isolation and separation of circulating tumor cells (CTCs) from peripheral blood without compromising their viability is crucial for cancer diagnostics and prognosis. However, the successful isolation of CTCs is often quite challenging due to their low concentrations and size overlap with other blood cells. Microfluidics devices incorporating inertial forces in recent times have emerged as a promising tool for CTC separation with high throughput and minimal invasiveness. Despite these advantages, CTC isolation using inertial microfluidic devices still faces challenges in practical application due to their inability to separate CTCs having overlapping sizes with WBCs. To, tackle this issue, the present study offers a curved contraction-expansion structured inertial microfluidic device equipped with DEP, that possess the potential of continuous and high throughput separation of CTCs from WBCs regardless of their size overlap. The use of DEP force ensures the successful separation of similarly sized CTCs from WBCs from blood samples, and the use of a contraction-expansion structure offers precise microenvironment that enables the efficient use of DEP force for continuous label-free separation. The characteristics of cell transport and cell positioning are quantified through coupled physics analyses to evaluate the effects of different parameters such as: the aspect ratio of the rectangular channel on contraction zones and the ratio of sheath and mixture flow on separation efficiency of the proposed device.

Keywords: Circulating tumor cells, Label-free separation, Contraction-expansion channel, Dielectrophoresis, Inertial microfluidics

NOMENCLATURE

CTC	Circulating Tumor Cell
WBC	White Blood Cell
DEP	Dielectrophoresis
AR	Aspect Ratio [Width/Height]

1. INTRODUCTION

Isolation of circulating tumor cells (CTC) from blood samples is a crucial step in clinical diagnosis and prognosis of cancer in human body[1]. CTCs carry essential biomarkers for cancer progression, that can offer requisite information to detect and stop the spread of secondary tumor formation (metastasis). Thus, successful detection and separation of CTCs from blood cells offers a key component in cancer research, since metastasis is the leading factor for the termination of 90% of cancer patients[2].

In recent times, microfluidic devices have emerged to be an excellent candidate to enable high throughput cell separations with greater separation efficiency. The technique utilized in majority of microfluidic devices are mainly categorized into two types: active and passive. Active methods use an external force field in the form of electrical[3], magnetic[4], and acoustic waves[5], to enable cell separation based on the inherent characteristic physical differences of CTCs from other blood cells. On the contrary, separation of cells can also be achieved with the help of their intrinsic properties such as density, size and deformability in passive methods. Furthermore, the channel geometry and the flow rate can also affect cell separation criteria for different passive methods of cell separation such as: pinch flow fractionation (PFF), deterministic lateral displacement (DLD)[6], [7], hydrodynamic filtration[8] and inertial methods [9] etc.

Among most other passive techniques, inertial migration of particles inside microchannels offer superior performance including high-throughput and label free separation along with simple geometric structure [10]. In inertial microfluidic devices, the randomly dispersed particles take equilibrium positions that are affected by various inertial forces acting on them. However, the equilibrium position taken by the particles are totally size dependent, thus inertial microfluidic devices can only separate cells depending on the dimensions of the particles[11]. It has been already reported by various researchers that, many white blood cells ((WBCs) overlap in size with CTCs present in blood samples that generate a major drawback of inertial microfluidics

in practical applications [12]. To tackle this challenge, it is required to couple active techniques with inertial devices to form a hybrid separation technique, that can offer alternatives to earlier mentioned limitations.

The performance of coupled microfluidic devices has been explored by a number of researchers. Kim et al.[13] presented an inertia-acoustophoresis hybrid microchannel that can achieve more than 99% of separation efficiency for 5 and 13 μm particles with throughput as high as 100 μL/min. Seo et al.[14] presented a hybrid cell sorter through combination of hydrodynamics and magnetophoresis where cells are separated by using magnetic susceptibility. But both of these models separate the cells of different size only. Zhang et al.[15] reported a novel DEP-inertial device capable of achieving a lateral separation distance of about 29 μm, but that also works when there is a significant size difference between the cells. Thus, these studies fail to overcome the limitations with overlapping sized CTCs with WBCs. Moreover, Aghamo et al.[16] combined DLD with DEP to separate similarly sized CTCs from WBCs in blood sample. It exhibits a low throughput of about 2 μL/min. Alazzam et al.[17] proposed a DEP-inertial microfluidic device designed to separate MDA-MB-231 CTCs from heterogenous mixture of blood cells. Their design also allows for only 6 μL/min of sample flow rate. It can be seen that; a few studies have been reported that has the capability to separate overlapping sized CTCs from WBCs having higher throughputs for faster sample processing.

Our group has previously reported a hybrid microfluidic device that has the potential to separate CTCs from similar-sized WBCs using a zigzag structure equipped with DEP forces [18]. Despite using DEP forces, the proposed device has a very low separation distance that can generate complexities for precise cell separation [19]. To tackle this issue, in a later work, we have presented a DEP enabled contraction-extraction structured inertial microfluidic device that can achieve as high as 233 μm lateral separation distance between circulating tumor cells from other blood cells [20]. The proposed device also offers a very high throughput that can be tuned for different applied voltage (DEP force) to achieve better separation efficiency of CTCs from similarly sized white blood cells. The reported study presented the effect of flow rate and applied voltage on the separation criteria of the device. It has been already reported that, the cell separation criteria inside inertial devices are greatly dependent on channel dimensions[21]. It is necessary to study the effects of channel aspect ratio of the curved geometry of any to fully understand the design aspects. On the other hand, to handle large amount of blood samples, the throughput of device is a parameter of great interests. Thus, in order to obtain an overall understanding of the device presented, this study presents the effects of rectangular channel aspect ratio and the mixture to sheath flow ratio on CTC separation from blood samples.

2. THEORETICAL BACKGROUND

2.1 Inertial migration

Inertial microfluidics functions on the principle of particle lateral migration inside fluid fields to reach equilibrium positions[21]. Typically, in a micro-scale channel device, Reynolds number ranges from 1 to 100[10]. In straight channels, particles migrate under inertial lift force, that includes wall-induced lift force and shear gradient lift force. The resultant lift force on the particles can be expressed as[22], [23] :

$$F_L = \frac{f_L\,(Re,\ z)\rho_f U_m^2 a_p^4}{D_h^2} \quad (1)$$

$$Re = \frac{\rho_f U_m D_h}{\mu} \quad (2)$$

where ρ_f, U_m, μ, a_p, D_h, and f_L are fluid density, the maximum velocity of the fluid, dynamic viscosity, cell diameter, the hydraulic diameter of the channel, and lift coefficient, respectively. The lift coefficient, f_L, depends on the channel Reynolds number (Re) and vertical position (z) within the channel cross-section. It remains almost constant for $Re < 100$ and its approximate value is 0.5 in most cases[24].

In curved channels, particles also experience a drag force due to the Dean flow (secondary flow) in the channel cross section. This generates due to the presence of curvature downstream of fluid flow, that creates a centrifugal force radially outward resulting in two counter-rotating vortices termed as Dean vortices. The Dean number can be expressed by[25]:

$$De = \frac{\rho_f U_m D_h}{\mu}\sqrt{\frac{D_h}{2R}} \quad (3)$$

where R is the radius of the curvature of the channel. The Dean flow introduces a force known as the Dean drag force (F_{Dean}) which is expressed as[26]:

$$F_{Dean} = 5.4 \times 10^{-4}\pi\mu a_p (De)^{1.63} \quad (4)$$

where a_p is the radius of the particle. The combination of both the Dean drag force and inertial lift force determines the number of equilibrium positions of particles or cells.

2.2 Dielectrophoresis

When particles in a fluid medium experience electric force due to interactions between non-uniform electric fields and field-induced electrical polarization of particles, the force is termed as Dielectrophoretic (DEP) force. The particles emerged in an alternating electric field will be affected by a time averaged DEP force given by[27]:

$$F_{DEP} = 2\pi\varepsilon_{med} a_p^3 Re[K_{CM}(f)]\nabla E^2 \quad (5)$$

where ε_{med} and f are the permittivity of the suspension medium and the frequency of the applied non-uniform electric field of strength E respectively. It can be noted from equation (5), if $Re[K_{CM})] > 0$, the DEP force is positive and particles are attracted to the regions of strong electric fields, while if $Re[K_{CM})] < 0$, the DEP force is negative and the particles are repelled opposite the regions of electric fields.

The term $Re[K_{CM}(f)]$ reflects the magnitude of the real part of the Clausius-Mossotti (CM) factor that is defined by:

$$K_{CM}(f) = \frac{\bar{\varepsilon}_{cell} - \bar{\varepsilon}_{med}}{\bar{\varepsilon}_{cell} + 2\bar{\varepsilon}_{med}} \quad (6)$$

where $\bar{\varepsilon}_{cell}$ and $\bar{\varepsilon}_{med}$ are complex permittivity of cell and medium, respectively, and both of them are the function of the applied frequency.

In the present work, an array of interdigitated electrode (IDE) was patterned on the inner side walls of the contraction

zones of a contraction-expansion structured curved microfluidic device to generate a negative DEP (n-DEP) on the particles and push them towards outer the outer wall. Since the DEP force in the horizontal and vertical direction is too weak to alter particle positions due to a high flow speed, the lateral DEP force (F_{DEPy}) counteracts with the lift force generated due to inertial effects along lateral directions. The DEP force in the whole manuscript indicates the DEP force component in the lateral (y) direction.

2.3 Particle separation mechanism in DEP enabled curved contraction expansion microchannel

The present study offers a curved array of contraction-expansion microchannel having the potential to separate the CTCs from WBCs from blood samples regardless of their size overlap. Due to fluid stream, shear induced lift force is generated throughout the channel, that pushes the cells toward the outer wall from the channel center. Additionally, the wall induced lift force acts in the opposite direction and pushes the cells towards channel center. A sharp cross-sectional area modification along the flow direction makes the fluid stream follow a curved path. Since, smaller particles are strongly influenced by forces due to dean flow, these particles tend to move towards the outer wall of the curved geometry, while the larger particles experience greater shear induced lift force, pushing them to reach inner wall of the channel. Thus, complete size-based separation can be achieved by the contraction-expansion structured microfluidic device without the use of DEP force.

It has been introduced earlier that shear-induced lift force is stronger in the contraction regions due to the flow acceleration in the contraction region[28]. That is why, in our design, the interdigitated electrode arrays are placed outside of the inner wall of the contraction region to generate DEP force in the lateral direction to counter the shear induced lift force of targeted particles to obtain successful separation of CTCs from identical sized WBCs. A sheath flow pinches the particles towards the inner side walls of the channel. AC electric field having a cross over frequency of CTCs is utilized when the cells are reached near the inner side of the contraction region. The equilibrium position obtained by different particles will be governed by the strength of the lift force, F_L, and DEP force, F_{DEP}. Due to the cross over frequency adjustments, CTCs experiencing negligible DEP forces, reaches the equilibrium positions based on the lift forces towards the inner wall of the channel. WBCs will strongly get affected by the DEP force and will attain an equilibrium position towards the outer wall of the channel, generating a successful separation regardless of their identical dimensions.

3. WORKING MODEL

The curved contraction expansion structured microchannel consists of rectangular shaped channel. The inner and outer radius of the curvature is 2150 µm and 2500 µm respectively, having a width 350 µm on the expansion zones. The width of the channel on contraction zones is adjusted from 25 to 200 µm. The height of the channel is considered 50 µm.

There are two inlets separated at the inlet to introduce mixture and sheath flow. As presented in figure 1, the sheath flow is used to pinch the cells towards the inner wall of the channel. In all of the study, the sample flow is kept constant at 10 µL/min and the sheath flow is adjusted on a range of values to study the effect of the sheath flow and mixture flow ratio on the cell separation efficiency.

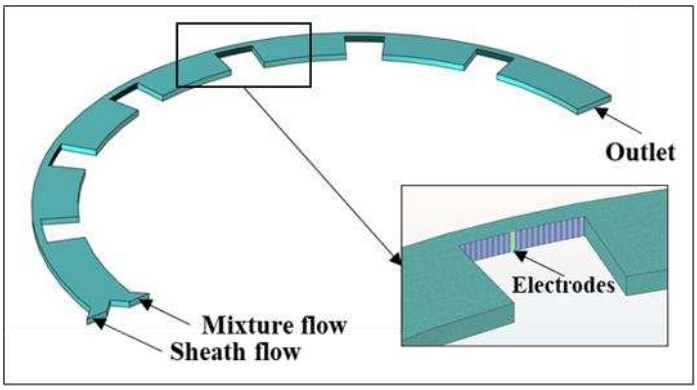

FIGURE 1: WORKING MODEL OF THE CURVED CONTRACTION EXPANSION STRUCTURED MICROFLUIDIC DEVICE.

In this study, A549 cells and Granulocytes are considered as representatives of CTCs and WBCs respectively. Since, Granulocytes has a significant size overlap with CTCs and they also have a large abundance in human body, their selection justifies a wide range of practical applications. Since, the size of CTCs are usually larger than WBCs, smaller sized WBCs are also used in this analysis to demonstrate the separation capacity of the presented device regardless of the dimensions of the cells. The cell properties regarding the dimensions and dielectric properties are presented in table 1.

TABLE 1
DIELECTRIC PROPERTIES OF THE CELL BEADS WITH MEDIUM CONDUCTIVITY OF 0.055 S/M AND RELATIVE PERMITTIVITY OF 80 FOR BOTH CTCS AND WBCS.

Cell type	Radius r (µm)	Crossover frequency f_c (kHz)	Cytoplasm conductivity σ_{cp} (S/m)	Cytoplasm complex permittivity $\bar{\varepsilon}_{cp}$	Membrane thickness D (nm)	Membrane conductivity σ_m (S/m)	Membrane complex permittivity $\bar{\varepsilon}_m$
A-549 CTCs	7.75±0.25	65±2.5	0.99	100	10	2×10^{-6}	27
Similar-sized WBCs (Granulocytes)	7.75±0.1	156.65±2	0.72	111	5	1×10^{-6}	5.54
Different-sized WBCs (Lymphocytes)	3.75±0.25	325±21	0.72	111	5	1×10^{-6}	5.54

As discussed in the theory sections, the Clausius-Mossotti (CM) factor that depends on the applied frequency dictates if positive DEP (pDEP), negative DEP (nDEP), or zero DEP force work on a particular type of cells. In our analysis, we device it such a way that a negative DEP force acts upon the white blood cells to push them towards the outer side walls, and the CTCs will experience zero DEP force as the frequency applied is set to

the cross over frequency of CTCs. Figure 2 presents the change of CM factor against a range of applied frequencies and the mean CTC cross-over-frequency is shown by the vertical line that is 65 kHz.

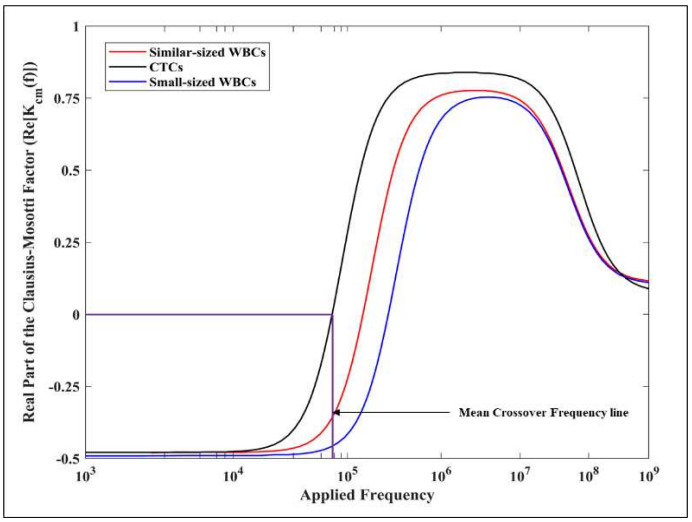

FIGURE 2: THE REAL PART OF CLAUSIUS-MOSSOTTI FACTOR AT DIFFERENT APPLIED FREQUNECY THAT DETERMINES THE NATURE OF DEP FORCE ACTING ON PARTICLES. THE CROSS-OVER FREQUENCY IS MARKED WITH BLACK COLOUR.

4. NUMERICAL MODEL

In order to model fluid flow, electric field and cell separation, COMSOL 6.0 is used in the current study. AC/DC module of COMSOL 6.0 is used to solve the electric field generated by the electrodes. The velocity field is solved initially through laminar flow module that solves the following Navier-Stokes equations accompanied with continuity equation,

$$\rho\left[\frac{\partial v}{\partial t} + v \cdot \nabla v\right] = \nabla \cdot [-pI + \mu(\nabla v + (\nabla v)^T)] + F_v \quad (7)$$

$$\nabla \cdot v = 0 \quad (8)$$

where ρ, v, μ and p are the fluid density, velocity, viscosity, and pressure, respectively. Here, F_v denotes the volume force which is created by the fluid-cell interaction.

The following equations are solved to obtain the electric field,

$$E = -\nabla\phi \quad (9)$$

$$\nabla \cdot (\varepsilon_m E) = \rho_E \quad (10)$$

$$\frac{\partial \rho_E}{\partial t} + \nabla \cdot (\sigma E) = 0 \quad (11)$$

Where ϕ, ε_m, ρ_E and σ are the electric potential, medium permittivity, net volumetric free charge density, and medium conductivity, respectively.

While passing through the channel, the cells are affected by the combined effects of lift, drag, sedimentation, basset and DEP forces. The net number of forces acting on a particle determines the trajectory of the cells. To account for the effects of these forces while travelling through the channel Newton's second law is applied by the transient solver to solve for their motion in fluid domain. The following equation of motion is solved by the transient solver,

$$m_{cell}\frac{d}{dt}(v_{cell}) = F_{Drag} + F_{Lift} + F_{DEP} + F_{Sedim} + F_{Basset} \quad (12)$$

To evaluate drag force on the particles, the Schiller-Naumann drag model is used,

$$F_{Drag} = \left(\frac{1}{\tau_p}\right)m_{cell}(u - v_{cell}) \quad (13)$$

Where, u is the fluid velocity. The term τ_p represent velocity response time that is defined by:

$$\tau_p = \frac{4\rho_p d^2}{3\mu C_d Re} \quad (14)$$

Where, ρ_p, C_d and d are cell density, drag coefficient, and cell diameter, respectively. A particle passing through a fluid domain, generates a lagging boundary layer with the change of relative velocity (acceleration). This lagging boundary layer development causes the Basset force to origin accounting for the viscous effects of the fluid. In our analysis, the ratio of the fluid and particle density being very small, the basset force is quite negligible compared to the drag force (the medium density, ρ_m = 1000 kg/m^3 and cell density, ρ_p = 1050 kg/m^3)[29]. Since, densities of cell and medium are very close to each other, we can also ignore the sedimentation force in the current study. The volume force mentioned earlier is created due to fluid/cell interaction that equals the total drag force and acts in the opposite direction to the drag force. The volume force is expressed as:

$$F_V(r) = -\sum_{i=1}^{n} F_{Drag,i}\,\delta(r - q_i) \quad (15)$$

Where r, δ, q_i, and n are the position of the cell, Dirac delta function, position vector, and the total number of cells, respectively. DEP force formed through non-uniform electric field can be obtained from equation (5). However, the cells contain different elements such as cytoplasm, cell nucleus, and cell membrane that determines the dielectric behavior of cells. To characterize the biological cells, an equation derived from single shell model can be used equivalent of complex permittivity of cells[30]:

$$\bar{\varepsilon}_{cell} = \bar{\varepsilon}_m \frac{\left(\frac{r}{r-d}\right)^3 + 2\left(\frac{\bar{\varepsilon}_i - \bar{\varepsilon}_m}{\bar{\varepsilon}_i + \bar{\varepsilon}_m}\right)}{\left(\frac{r}{r-d}\right)^3 - \left(\frac{\bar{\varepsilon}_i - \bar{\varepsilon}_m}{\bar{\varepsilon}_i + \bar{\varepsilon}_m}\right)} \quad (16$$

Where r, d, $\bar{\varepsilon}_m$, $\bar{\varepsilon}_i$, and $\bar{\varepsilon}_{cell}$ are the cell radius, membrane thickness, complex permittivity of the membrane, the complex permittivity of cytoplasm, and equivalent complex permittivity of the cell, respectively. In order to solve the numerical model, GMRES solver is used.

5. RESULTS AND DISCUSSION

The findings from thorough examination of our presented microfluidic device consisting of a number of contraction-expansion structure on separation performance are presented in this section. The first sub-section deals with the validation of the numerical model used in this study. The later sub-sections present further scrutiny of channel aspect ratio and mixture to sheath flow ratio to determine optimum design criteria of our device.

5.1 Validation of the numerical model

The numerical model used in this study is compared with results presented in Lee et al. [31]. As presented in figure 3, the probability density of particle position from the simulation is closely aligned with the experiments. It is also found out that the correlation coefficient and root mean square error (RMSE) between the experiment and simulation are 0.87 and 0.07 respectively. That suggests the data from our numerical model significantly aligns with the experiments.

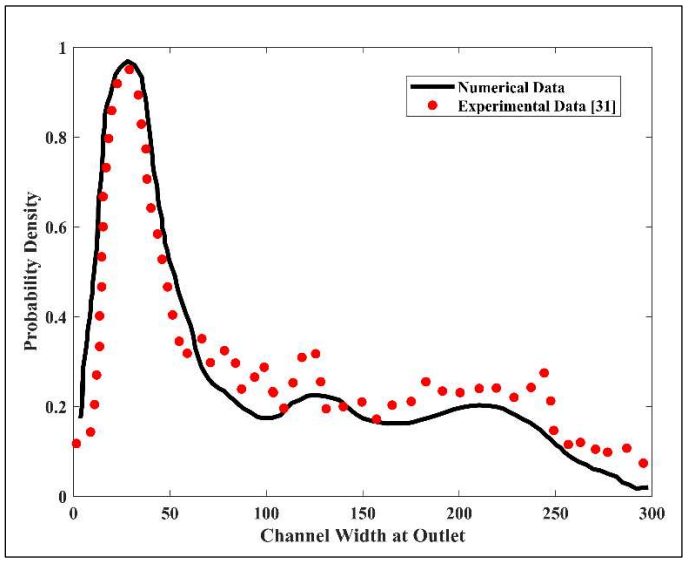

FIGURE 3: COMPARISON BETWEEN DATA FROM NUMERICAL SIMULATIONS AND EXPERIMENTAL REPORTED BY LEE ET AL. [31]

5.2 Effects of the rectangular channel aspect ratio

This section presents the effects of aspect ratio of the rectangular shaped channel on cell separation. As presented by Cruz and Hjort [32], the cell separation characteristics in a microfluidic device is strongly affected by the channel aspect ratio. In our proposed design, the particles experience greater shear gradient lift and secondary drag forces in the contraction region of the device. Thus, the aspect ratio of the channel on the contraction region is the parameter of interest to design contraction-expansion structured microfluidic devices targeted to cell separation.

From figure 4, the lateral position of cells at outlet is greatly impacted by the aspect ratio of the channel at the contraction region. An aspect ratio of 1 with equal height and width of 50 µm, offers maximum separation distance between CTCs and the WBCs. Higher aspect ratio channels are obtained through increasing the width of the contraction area. Since, our model contains electrodes placement at the sidewalls of the channel, the effect of DEP force greatly depends upon the channel width. By increasing the width more, the effects of DEP forces are seen deteriorating. And, when the DEP force is not strong enough to counter the lift forces, the larger particles (CTCs and similar sized WBCs) get focused together and the device shows size-based separation. This also presents the capability of the curved contraction-expansion device to generate size-based separation in a high aspect ratio channel.

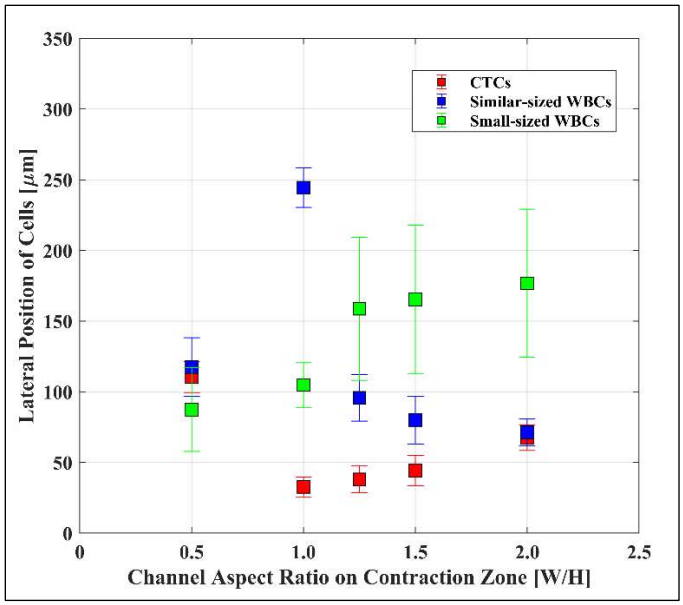

FIGURE 4. LATERAL POSITION OF CELLS AT THE OUTLET VS RECTANGULAR CHANNEL ASPECT RATIO.

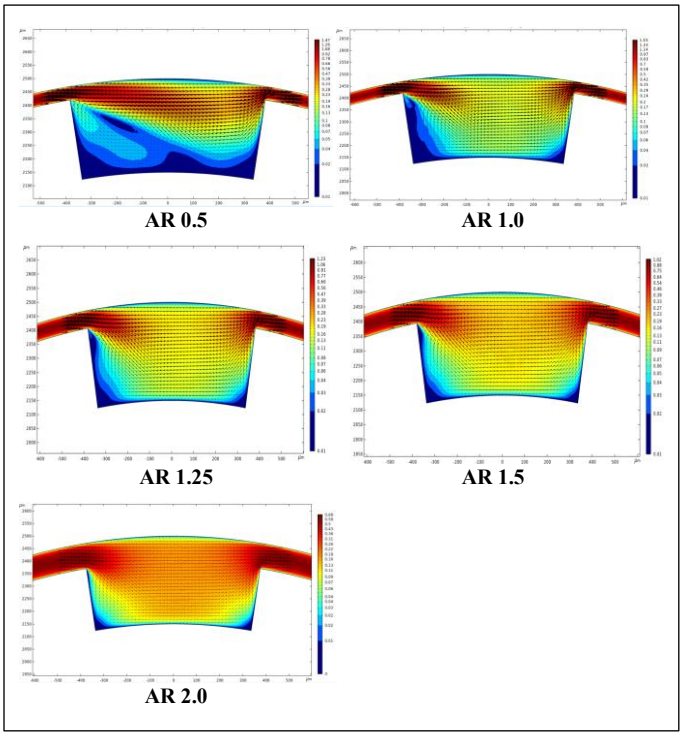

FIGURE 5. HORIZONTAL VELOCITY DISTRIBUTION IN CONTRACTION REGION WITH DIFFERENT CHANNEL ASPECT RATIO.

In order to study the separation techniques of the curved contraction expansion channel at different aspect ratio, velocity vectors at contraction-expansion-contraction entrance are

presented in figure 5. At very small aspect ratio, a small vortex is seen in the expansion zone due to sudden increase in area, that is not suitable for efficient inertial separation. This phenomenon is consistent with experimental works reported in [33]. On the other hand, higher aspect ratio channels are more suitable for inertial separation since small and larger particles get precise focusing along the streamline.

5.3 Effects of the mixture to sheath flow ratio

This section reports the effect of mixture to sheath flow ratio on the separation efficiency of CTCs from white blood cells. The mixture flow rate is kept constant at 10 µL/min and 50-volt electric potential is applied on the electrodes. Sheath flow is adjusted from 10 µL/min to 200 µL/min that results in a ratio of 1:1 to 1:20, to test the sheathing effect on high throughput cell separation criteria. It has been observed from the study that, a mixture to sheath flow ratio of 1:10 provides highest separation distance between the circulating tumor cells from the white blood cells with a very narrow distribution of cells on the lateral position in the outlets. This point acts as a pivoting position for the analysis as increasing or decreasing the ratio results in poor separation distances between the set of cells from the mixture.

The effect of mixture to sheath flow ratio is critical in order to obtain better separation efficiency and high throughput. A higher sheath to mixture flow ratio generates more wall induced lift force within the channel that overcomes the lateral DEP force, and thus, larger white blood cells tend to move towards the inner side wall of the channel, causing the focusing distance of CTCs and WBCs to get reduced. On the other hand, large sheath to mixture flow ratio causes the smaller WBCs to acquire different focusing positions due to variation in the lift forces with increased flow velocity.

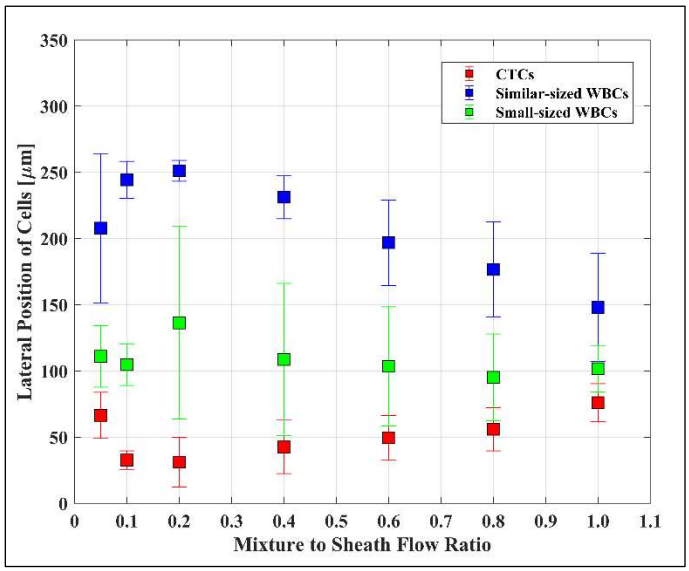

FIGURE 6. LATERAL POSITION OF CELLS AT THE OUTLET AT DIFFERENT MIXTURE TO SHEATH FLOW RATIO.

6. CONCLUSION

This study presents a curved contraction-expansion structured hybrid microfluidic device having the potential of separating CTC from other blood cells regardless of their size. The effects of aspect ratio of the rectangular channel on cell separation characteristics are presented to propose a design and application guidelines for similar devices. The cell separation performance of the device is also investigated on the ratio of the mixture to sheath flow ratio. It has been found that, an aspect ratio of 1 in the contraction region with mixture to sheath flow ratio of 10:1 produces maximum lateral cell separation in the device. The results presented through the analysis will layout the guidelines to applying contraction-expansion based hybrid microfluidic device for targeted cancer cell separation techniques.

ACKNOWLEDGEMENT

This material is based upon work supported by the National Science Foundation under Grant No. 1917299.

REFERENCES

[1] M. Toner and D. Irimia, “Blood-on-a-Chip,” *Annu. Rev. Biomed. Eng.*, vol. 7, no. 1, pp. 77–103, Aug. 2005, doi: 10.1146/annurev.bioeng.7.011205.135108.

[2] M. Cristofanilli *et al.*, “Circulating Tumor Cells, Disease Progression, and Survival in Metastatic Breast Cancer,” *N. Engl. J. Med.*, vol. 351, no. 8, pp. 781–791, Aug. 2004, doi: 10.1056/NEJMoa040766.

[3] F. Yang *et al.*, “Extraction of Cell-Free Whole Blood Plasma Using a Dielectrophoresis-Based Microfluidic Device,” *Biotechnol. J.*, vol. 14, no. 3, p. 1800181, Mar. 2019, doi: 10.1002/biot.201800181.

[4] M. Hejazian, W. Li, and N.-T. Nguyen, “Lab on a chip for continuous-flow magnetic cell separation,” *Lab. Chip*, vol. 15, no. 4, pp. 959–970, 2015, doi: 10.1039/C4LC01422G.

[5] H. Ahmed *et al.*, “A Pumpless Acoustofluidic Platform for Size-Selective Concentration and Separation of Microparticles,” *Anal. Chem.*, vol. 89, no. 24, pp. 13575–13581, Dec. 2017, doi: 10.1021/acs.analchem.7b04014.

[6] M. Rahmati and X. Chen, “Separation of circulating tumor cells from blood using dielectrophoretic DLD manipulation,” *Biomed. Microdevices*, vol. 23, no. 4, p. 49, Sep. 2021, doi: 10.1007/s10544-021-00587-8.

[7] A. Aghilinejad, M. Aghaamoo, and X. Chen, “On the transport of particles/cells in high-throughput deterministic lateral displacement devices: Implications for circulating tumor cell separation,” *Biomicrofluidics*, vol. 13, no. 3, p. 034112, May 2019, doi: 10.1063/1.5092718.

[8] M. Yamada, M. Nakashima, and M. Seki, “Pinched Flow Fractionation: Continuous Size Separation of Particles Utilizing a Laminar Flow Profile in a Pinched Microchannel,” *Anal. Chem.*, vol. 76, no. 18, pp. 5465–5471, Sep. 2004, doi: 10.1021/ac049863r.

[9] A. A. S. Bhagat, S. S. Kuntaegowdanahalli, and I. Papautsky, “Enhanced particle filtration in straight microchannels using shear-modulated inertial migration,”

Phys. Fluids, vol. 20, no. 10, p. 101702, Oct. 2008, doi: 10.1063/1.2998844.

[10] W. Tang, S. Zhu, D. Jiang, L. Zhu, J. Yang, and N. Xiang, "Channel innovations for inertial microfluidics," *Lab. Chip*, vol. 20, no. 19, pp. 3485–3502, 2020, doi: 10.1039/D0LC00714E.

[11] S. S. Kuntaegowdanahalli, A. A. S. Bhagat, G. Kumar, and I. Papautsky, "Inertial microfluidics for continuous particle separation in spiral microchannels," *Lab. Chip*, vol. 9, no. 20, pp. 2973–2980, Oct. 2009, doi: 10.1039/B908271A.

[12] D. Marrinucci, K. Bethel, M. Luttgen, R. H. Bruce, J. Nieva, and P. Kuhn, "Circulating Tumor Cells From Well-Differentiated Lung Adenocarcinoma Retain Cytomorphologic Features of Primary Tumor Type," *Arch. Pathol. Lab. Med.*, vol. 133, no. 9, pp. 1468–1471, Sep. 2009, doi: 10.5858/133.9.1468.

[13] U. Kim, B. Oh, J. Ahn, S. Lee, and Y. Cho, "Inertia–Acoustophoresis Hybrid Microfluidic Device for Rapid and Efficient Cell Separation," *Sensors*, vol. 22, no. 13, p. 4709, Jun. 2022, doi: 10.3390/s22134709.

[14] H.-K. Seo, Y.-H. Kim, H.-O. Kim, and Y.-J. Kim, "Hybrid cell sorters for on-chip cell separation by hydrodynamics and magnetophoresis," *J. Micromechanics Microengineering*, vol. 20, no. 9, p. 095019, Sep. 2010, doi: 10.1088/0960-1317/20/9/095019.

[15] J. Zhang *et al.*, "Tunable particle separation in a hybrid dielectrophoresis (DEP)- inertial microfluidic device," *Sens. Actuators B Chem.*, vol. 267, pp. 14–25, Aug. 2018, doi: 10.1016/j.snb.2018.04.020.

[16] M. Aghaamoo, A. Aghilinejad, X. Chen, and J. Xu, "On the design of deterministic dielectrophoresis for continuous separation of circulating tumor cells from peripheral blood cells," *ELECTROPHORESIS*, vol. 40, no. 10, pp. 1486–1493, May 2019, doi: 10.1002/elps.201800459.

[17] A. Alazzam, B. Mathew, and F. Alhammadi, "Novel microfluidic device for the continuous separation of cancer cells using dielectrophoresis: Alazzam et al.," *J. Sep. Sci.*, vol. 40, no. 5, pp. 1193–1200, Mar. 2017, doi: 10.1002/jssc.201601061.

[18] M. Khan and X. Chen, "Numerical study of dielectrophoresis-modified inertial migration for overlapping sized cell separation," *ELECTROPHORESIS*, vol. 43, no. 7–8, pp. 879–891, 2022, doi: 10.1002/elps.202100187.

[19] M. S. Islam, M. R. Uddin, and X. Chen, "Circulating Tumor Cell Separation in a Zigzag Channel Using Dielectrophoresis Based Inertial Microfluidics," in *Volume 8: Fluids Engineering; Heat Transfer and Thermal Engineering*, Columbus, Ohio, USA: American Society of Mechanical Engineers, Oct. 2022, p. V008T10A014. doi: 10.1115/IMECE2022-95384.

[20] M. S. Islam and X. Chen, "Continuous CTC separation through a DEP -based contraction–expansion inertial microfluidic channel," *Biotechnol. Prog.*, p. e3341, Mar. 2023, doi: 10.1002/btpr.3341.

[21] D. Di Carlo, "Inertial microfluidics," *Lab. Chip*, vol. 9, no. 21, p. 3038, 2009, doi: 10.1039/b912547g.

[22] E. S. Asmolov, "The inertial lift on a spherical particle in a plane Poiseuille flow at large channel Reynolds number," *J. Fluid Mech.*, vol. 381, pp. 63–87, Feb. 1999, doi: 10.1017/S0022112098003474.

[23] D. Di Carlo, J. F. Edd, K. J. Humphry, H. A. Stone, and M. Toner, "Particle Segregation and Dynamics in Confined Flows," *Phys. Rev. Lett.*, vol. 102, no. 9, Art. no. 9, Mar. 2009, doi: 10.1103/PhysRevLett.102.094503.

[24] D. Di Carlo, D. Irimia, R. G. Tompkins, and M. Toner, "Continuous inertial focusing, ordering, and separation of particles in microchannels," *Proc. Natl. Acad. Sci.*, vol. 104, no. 48, pp. 18892–18897, Nov. 2007, doi: 10.1073/pnas.0704958104.

[25] W. R. Dean, "Fluid motion in a curved channel," *Proc. R. Soc. Lond. Ser. Contain. Pap. Math. Phys. Character*, vol. 121, no. 787, pp. 402–420, Nov. 1928, doi: 10.1098/rspa.1928.0205.

[26] J. Zhu, T.-R. J. Tzeng, and X. Xuan, "Continuous dielectrophoretic separation of particles in a spiral microchannel," *ELECTROPHORESIS*, vol. 31, no. 8, pp. 1382–1388, Apr. 2010, doi: 10.1002/elps.200900736.

[27] T. B. Jones, *Electromechanics of Particles*, 1st ed. Cambridge University Press, 1995. doi: 10.1017/CBO9780511574498.

[28] M. G. Lee, S. Choi, and J.-K. Park, "Inertial separation in a contraction–expansion array microchannel," *J. Chromatogr. A*, vol. 1218, no. 27, pp. 4138–4143, Jul. 2011, doi: 10.1016/j.chroma.2010.11.081.

[29] W. Waheed, O. Z. Sharaf, A. Alazzam, and E. Abu-Nada, "Dielectrophoresis-field flow fractionation for separation of particles: A critical review," *J. Chromatogr. A*, vol. 1637, p. 461799, Jan. 2021, doi: 10.1016/j.chroma.2020.461799.

[30] D. Kim, M. Sonker, and A. Ros, "Dielectrophoresis: From Molecular to Micrometer-Scale Analytes," *Anal. Chem.*, vol. 91, no. 1, pp. 277–295, Jan. 2019, doi: 10.1021/acs.analchem.8b05454.

[31] M. G. Lee *et al.*, "Inertial blood plasma separation in a contraction–expansion array microchannel," *Appl. Phys. Lett.*, vol. 98, no. 25, p. 253702, Jun. 2011, doi: 10.1063/1.3601745.

[32] J. Cruz and K. Hjort, "The upper limit and lift force within inertial focusing in high aspect ratio curved microfluidics," *Sci. Rep.*, vol. 11, no. 1, p. 6473, Mar. 2021, doi: 10.1038/s41598-021-85910-2.

[33] J.-S. Park and H.-I. Jung, "Multiorifice Flow Fractionation: Continuous Size-Based Separation of Microspheres Using a Series of Contraction/Expansion Microchannels," *Anal. Chem.*, vol. 81, no. 20, pp. 8280–8288, Oct. 2009, doi: 10.1021/ac9005765.